

BALLISTIC ENERGY CONVERSION

Jan C.T. Eijkel¹, Albert van den Berg¹, and Yanbo Xie²

¹BIOS/Lab on a Chip group, MESA+ Institute for Nanotechnology and
Max Planck Center for Complex Fluid Dynamics, Twente University, NETHERLANDS

²MOE Key Laboratory of Space Applied Physics and Chemistry, School of Science,
Northwestern Polytechnical University, CHINA

ABSTRACT

Ballistic energy conversion is the direct conversion of kinetic energy into electrical energy. Aqueous droplet-based platforms are eminently suitable for this method, as droplets can be conveniently supplied with both kinetic energy and electrical charge. Starting with the 19th century gravity-driven Kelvin thunderstorm and the electrostatic generators of Melcher and Zahn from the 1960s, we describe the recent development of ballistic energy conversion both in experiment and theory. With this method experimental efficiencies of 48% have been reached at 20 kV operating voltage with an extremely simple setup. Theory predicts maximal efficiencies of more than 90%, operation at <100 Volt. Downscaling also promises to remove one of the largest disadvantages of electrostatic generators, namely the low power density: power densities of 1-1000 kW/m² are predicted.

KEYWORDS

Energy conversion, electrostatic generator

INTRODUCTION

Historically, electrostatic generators preceded electromagnetic generators by many years. Electrostatic generators operate by mechanically transporting charge to a high electrical potential. The charge is located at a surface where it is generated by the triboelectric effect (rubbing) or by induction by another high potential object. Since only little charge can reside on surfaces, the currents are typically low. On the other hand, objects can be charged to very high voltages, so voltages are typically high. Electrostatic generators are therefore still used for low current high voltage applications such as in particle physics. For almost all other practical purposes however, they were superseded by electromagnetic generators, after the discovery of electromagnetic induction by Michael Faraday in 1832.

An iconic fluidic electrostatic generator was constructed by W. Thompson (Lord Kelvin) in 1867[1]. This device, also called ‘Kelvin’s thunderstorm’, is shown in figure 1. Under the influence of gravity, droplets fall from two openings in a water bath into two receiving vessels. These receiving vessels are connected to metal inductor rings located just below the opposite opening in the water bath. The operational principle of this device is a positive feedback mechanism by repeated induction of charge on the falling droplets. Once a small imbalance in charge has caused one of the receiving vessels to acquire a net electrical charge, it will also charge the metal inductor ring which will induce the opposite charge on the droplet falling into the other receiving vessel. This positive

feedback process proceeds until the falling droplets and the receiving vessels become charged up to high potential. At very high potentials (10-20 kV) the process limits itself by charge leakage to the surroundings or sparking. Kelvin’s thunderstorm was extensively used as a didactic tool, for example in the lectures of Melcher and Zahn at MIT in the 1960s [2]. A large demonstration model was built which is still at display in the MIT and which is briefly mentioned by Zahn in his obituary for Melcher [3]. A video where the device is demonstrated (amongst other demonstrations of electrostatics) is available ([4]).

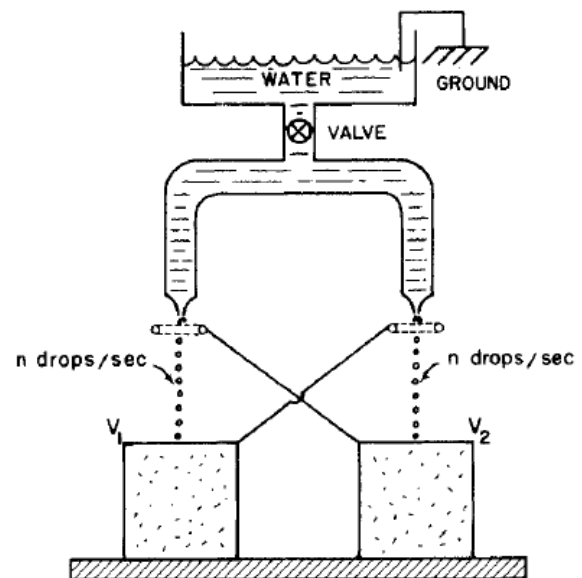


Figure 1 Schematic of the operational principle of Kelvin’s thunderstorm. Figure with permission from [5].

Interestingly, in the experimental setup of Zahn and Melcher the water is supplied from the mains and hence pressurized, but the consequences of using a pressurized supply instead of relying on the force of gravity as in Lord Kelvin’s original system were never analyzed, probably because the device was solely used for educational purposes.

An entirely independent line of investigation started in 1992, when Faubel and Steiner observed that an unexplained current was carried by a water microjet generated by high-pressure forcing of water through a micropore in a metal membrane [6]. Fifteen years later, Duffin and Saykally demonstrated that a similar setup (figure 2) could be applied for energy conversion [7,8]. They assumed that the phenomenon of streaming current was the origin of the observed current. Streaming current is generated when the ions in the double layer of the pore

are sheared away by the flowing liquid. They found a maximal energy conversion efficiency of 11%. For streaming-current-based systems this value is unexpectedly high, which they attributed to the non-developed flow-profile in the pore and to the absence of a (back) conduction current in the generated E-field, prevented by the discontinuous droplet stream.

In our work we have been further developing the above-cited work and, most importantly, have elucidated the mechanism of energy conversion. We showed that droplet kinetic energy played an essential role. On the basis of this theoretical understanding we further developed the method, which we termed ballistic energy conversion. We optimized the conversion efficiency and determined its theoretical limits [9,10,11].

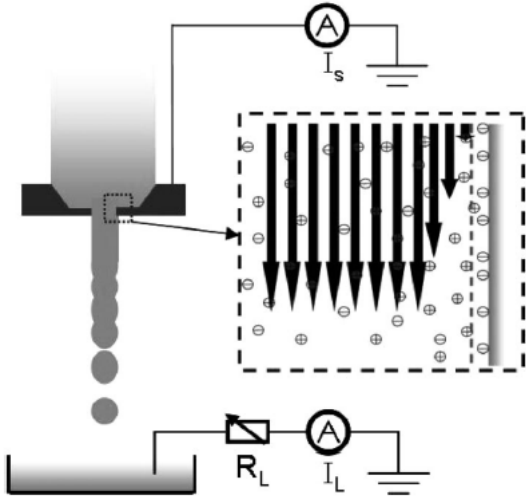


Figure 2 The experimental design of Duffin and Saykally [8]: a microjet carrying electrical charge is generated by pressure-forcing an aqueous jet through a micropore in a metal membrane. The charge is collected on a grounded target. Figure from ref [8] with permission.

THEORY – GENERAL

Common to all the water-based electrostatic generators mentioned in the introduction is, that a stream of droplets is used to transport charge to a target. The droplets originate from the water in the container. We can distinguish the different generators by their charge generation methods and droplet transport methods.

Table 1 subdivision of different fluidic electrostatic generators

	Air/water charge induction	Solid/water charge advection
Gravitational droplet transport	Kelvin [1]	
Inertial (ballistic) droplet transport	Melcher(?) [2], Xie [9]	Faubel, Duffin [6,8]

There are two ways of charge generation in the droplets: by advection of the mobile charge in the electrical double layer at the solid-water interface (streaming current), or by induction of charge at the air-water interface of the forming droplets (e.g. in Kelvin's

generator). We can furthermore distinguish two dominant forces to transport the droplets to the targets: gravity or inertia (ballistic). Table 1 provides an overview.

THEORY – DROPLET CHARGING

In the electrical double layer at the solid/water interface a large mobile charge density $\rho_e(r)$ resides, induced by the surface charge density (figure 3). When a flow is imposed, a charge transport in the flow direction results, called the streaming current. Since the charge is located close to the wall where the flow rate $v(r)$ is small, the streaming current is small. This current, which charges the droplets, is found by integrating the product of flow velocity and charge density over the pore radius,

$$I_s = \int_{r=a}^0 \rho_e(r)v(r)dr, \quad (1)$$

where r is the radial coordinate in the pore, a the pore radius, $\rho_e(r)$ the volume charge density in the electrical double layer and $v(r)$ the water velocity.

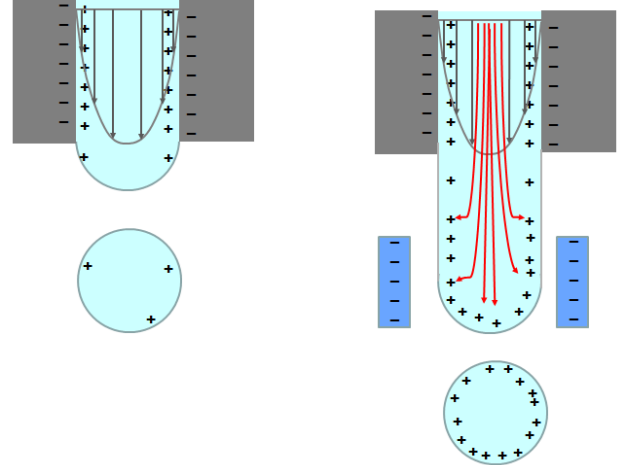


Figure 3 Left: Droplet charging by advection of EDL ions at the solid/liquid interface (streaming current); Right: Additional droplet charging by induction at the air/liquid interface using a gate electrode.

Charge can also be induced at the air/water interface (figure 3, right) using an external electrode. The maximal surface charge density of droplets in air is given by Rayleigh's limit, derived from the balance between inward surface tension and outward electrical pressure

$$q_d = 8\pi(\epsilon_0\gamma)^{0.5} a^{1.5}, \quad (2)$$

where ϵ_0 is the permittivity of vacuum, γ the surface tension and a the droplet radius. The maximal charge density at the air/water interface is much lower than the maximal charge density at the solid/water interface, because the EDL at the solid/water interface is stabilized by the counter-charge at the walls. Still, the droplet surface charge density that can be reached by air/water induction can be two orders of magnitude larger than in the case of the streaming current, because only a small

part of the EDL charge is advected into the droplet (equation 1). In the case of air/water charging, additional charges arrive in the droplets by conduction through the microjet (indicated by the red arrows in figure 3).

THEORY: CHARGED DROPLET TRANSPORT

Gravitational operation

In Kelvin's generator, surface tension dominates the droplet formation and large droplets form ($\sim 50 \mu\text{L}$). The charged droplets fall in the electrical field towards the receiving vessel charging it to high electrical potential. During the fall, the force balance on a droplet is

$$m_d g + q_d E + m_d a + F_{fr,d} = 0, \quad (3)$$

with m_d the droplet mass, g the acceleration due to gravity, q_d the droplet charge, E the electrical field, a the inertial acceleration and $F_{fr,d}$ the frictional force of the air on the droplet.

When we neglect the friction for the moment and assume that the droplet moves with a constant small velocity, the last two terms drop and we see that the electrical and gravitational forces are opposed on the droplet trajectory. Gravitational energy is thus converted to electrical energy. Integrating the forces over h , we obtain for the amount of energy converted per droplet:

$$W_{d,grav} = q_d U = m_d g h, \quad (4)$$

with U the target voltage. Two practical boundary conditions exist: droplets produced by dripping have $\sim 50 \mu\text{l}$ volume ($\sim 2.3 \text{ mm}$ in radius) and the maximal target voltage is 20 kV. The droplet size determines the maximal droplet charge/mass ratio according to the Rayleigh limit (equation 2) to

$$\frac{q_d}{m_d} = \frac{6}{\rho g} \frac{(\epsilon_0 \gamma)^{0.5}}{a^{1.5}}, \quad (5)$$

where ρ is the liquid density. Substituting the charge/mass ratio for droplets of 2.3 mm radius and the maximal target voltage $U = 20 \text{ kV}$ into equation 4, a maximal falling height h of 90 cm results. In practical conditions this is the longest trajectory that can be used to extract energy from a maximally charged 50 μL droplet. Every such droplet will then deposit 23 nC at a voltage of 20 kV, generating 460 μJ of electrical energy. Assuming a droplet generation frequency of 1 Hz, the generator power will be $\sim 0.5 \text{ mW}$ and the power density P_{den} about 1 W/m^2 , or 10 Joule/liter water.

Ballistic operation

The action of gravity to bring the droplets to the target can be replaced by inertia when the droplets are given high initial velocity. Instead of pitting the electrical force against gravity, we now pit it against inertia (Figure

4). When the deceleration a is much larger than the acceleration due to gravity the latter can be omitted and the force balance for each droplet on its air trajectory becomes

$$m_d a + q_d E + F_{fr,d} = 0. \quad (6)$$

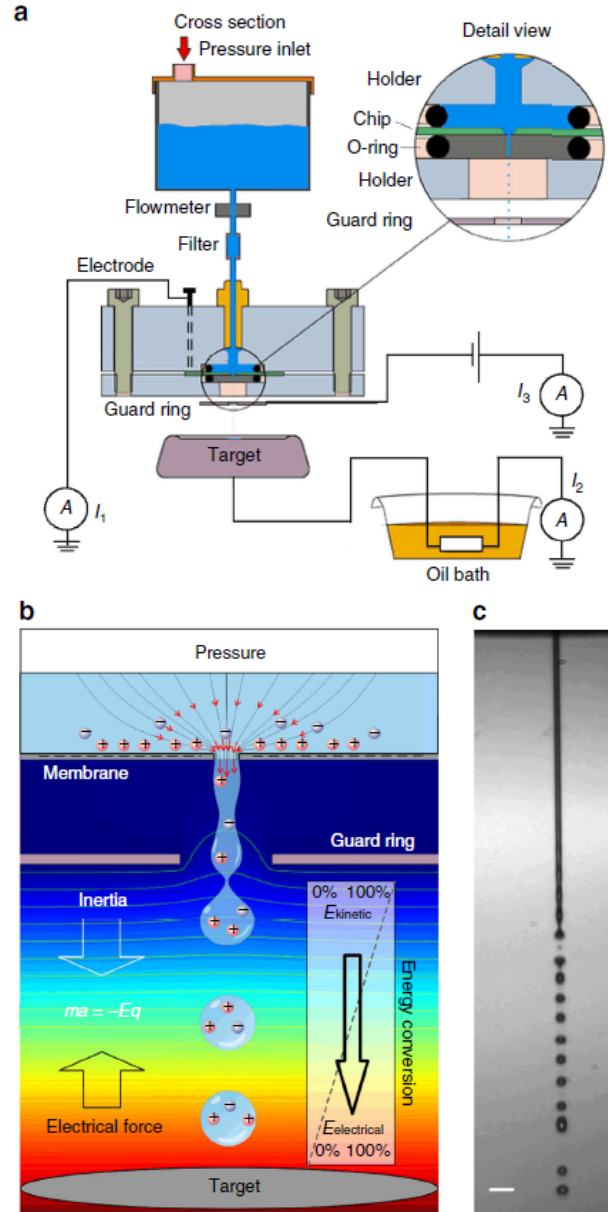


Figure 4 (a). Setup for ballistic energy generation; (b) Conceptual illustration of the conversion principle; (c) photomicrograph of the microjet. Figure from reference 10 with permission.

In the demonstrator of Zahn and Melcher, inertia probably played a role as pressure was applied from the waterworks to a droplet sprayhead [3,4]. The authors however seem to regard the sprayhead simply as a means to deliver the droplets to the collecting vessels and don't discuss the generation mechanism. Duffin and Saykally applied $\sim 100 \text{ bar}$ across a 5-20 μm diameter pore 100 μm thin membrane but similarly overlooked inertial effects in

their model. In our own experiments with ballistic energy conversion, we applied ~ 1 bar pressure over a very thin ($1 \mu\text{m}$) membrane. In all these three cases a jet is generated as inertia outweighs capillary forces (characterized by the Weber number $We = \rho av^2/\gamma > 4$)[11] at the pore exit. This jet subsequently breaks up into droplets. Jetting has two consequences: the droplet radius can become much smaller (\sim twice the pore radius) than with dripping and the droplets have high kinetic energy.

Our analysis was presented in [9]. In ballistic devices, the mechanism of energy conversion is less simple than in the case of Kelvin's droplet generator. We now need to consider a two-step process. First the pressure energy in the supplying water container is converted to kinetic energy of the droplets, and subsequently the kinetic energy of the droplets is converted to electrical energy on the droplet trajectory. For the first conversion process we can write from the Bernoulli equation

$$\frac{1}{2} m_d v_0^2 = (P - P_{loss}) V_d, \quad (7)$$

where v_0 is the initial droplet velocity, V_d the droplet volume, P the applied pressure and P_{loss} the part of the pressure energy that is dissipated by viscous forces and liquid jet surface creation [11].

On the droplet trajectory, neglecting the friction with the air and the contribution of gravity, we see from equation 6 that kinetic energy is converted to electrical energy. The amount of energy converted per droplet is

$$W_{d,ball} = q_d U = \frac{1}{2} m_d v_0^2, \quad (8)$$

There are again practical limits to the conversion. As the maximum practical target voltage U is 20 kV, there is a limit to the value of $m_d/q_d v_0^2$. To maximize v_0 and thus obtain a maximal energy per droplet, the charge over mass ratio must then be maximized. As the charge over mass ratio scales with $a^{-1.5}$ (equation 5), the use of microjets and microdroplets enables obtaining a higher energy per droplet. Alternatively, a high charge over mass ration can be used to operate the device at a lower voltage.

The top figure 5 shows in black the overall theoretical energy conversion efficiency of a ballistic converter, eff_{sys} , as a function of jet radius, as derived in reference 11. The theoretical efficiency can become more than 90% energy when larger droplets are used, since frictional losses decrease with increasing droplet size. The figure separately shows the efficiencies at the stages of droplet formation, eff_{kin} , dominated by liquid friction losses, and air transport, eff_{el} , dominated by air friction losses. The middle figure 5 shows that the power density of the converter at constant Weber number ($We = \rho av^2/\gamma$) decreases with jet radius. The main cause of this is a decrease of the input pressure that is needed to keep the Weber number constant and thereby maintain identical microjet behavior at increasing pore size. Bottom figure 5 shows the minimal target (generated) voltage needed to extract all kinetic energy for three Weber numbers.

Higher Weber numbers here imply higher applied pressures, which provide higher kinetic energy as well as necessitate higher target voltages for conversion. It can be seen that the possibility of operation at low operating voltages is predicted, albeit at lower power densities (figure 5 middle).

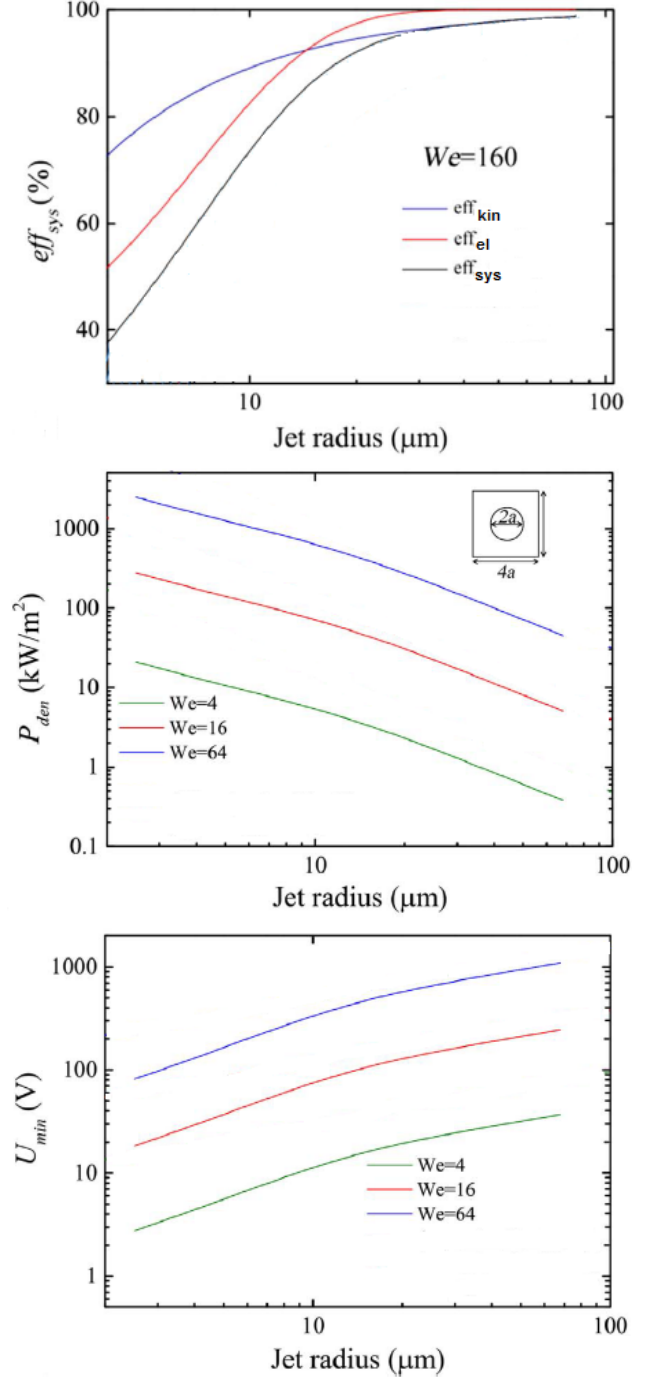


Figure 5 The theoretical efficiency (top), power density (middle) - assuming a $4a$ by $4a$ area for each pore-, and minimal operating voltage (bottom) of a microjet ballistic energy converter at three Weber numbers ($We = \rho av^2/\gamma$). Figures adapted from reference 11 with permission.

EXPERIMENTAL RESULTS

Xie et al. experimentally demonstrated conversion efficiencies of up to 48% with the device schematically shown in figure 4 [9]. They obtained the high efficiencies with a pore of 15 μm radius, an applied pressure of ~ 1 bar and a gate electrode ('guard ring' in figure 4) to induce additional charge on the water droplets. Figure 6 shows the efficiencies obtained as a function of the applied voltage on the gate electrode.

In a later modification, Xie et al. used a device with two microjets and applied the mutual induction method of Kelvin's droplet generator (figure 1). They also combined the device with a regulating electrical circuit to limit the inherent positive feedback of Kelvin's design that leads to instability and overcharging [10]. With this self-gating device efficiencies of 18% were obtained.

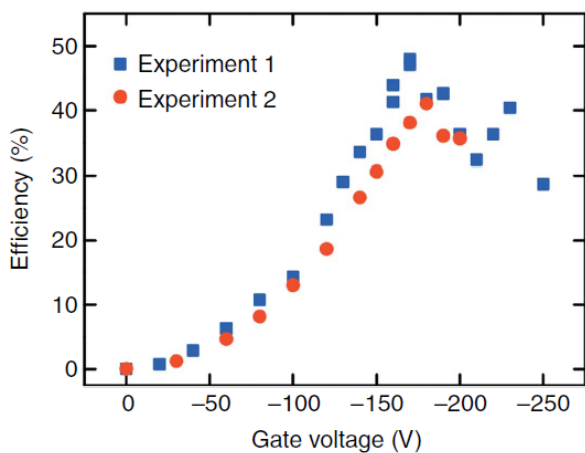


Figure 6 Experimentally obtained conversion efficiencies with the device shown in figure 4, as a function of voltage applied to the gate ('guard ring' in figure 4). Figure from reference 9 with permission.

COMPARISON OF GRAVITATIONAL AND BALLISTIC DEVICES

The same volume of water under practical conditions can generate much more power under ballistic operation than under gravitational operation. As shown above, under gravitational operation the falling height is limited to 90 cm while under ballistic operation pressures of several bars, equivalent to several 10s of meters of height, can be used. The generated power density (in W/m^3 water) can therefore be at least 20 times higher. Even more importantly, the gravitational system works by dripping at low Weber numbers, where droplets are large. The power density expressed per area of membrane therefore is not more than $10 \text{ W}/\text{m}^2$. In contrast, in ballistic operation the system operates by microjet breakup. Every microjet has a very small footprint, which theoretically allows power densities even surpassing $1 \text{ MW}/\text{m}^2$ (figure 5) by operating many microjets in parallel. The most important disadvantage of electrostatic generators with respect to electromagnetic generators is thereby removed. Finally, the distance between membrane and target can be made much smaller in ballistic operation as no action of gravity is needed, creating a much more

compact device. The higher charge/mass ratios of small droplets thereby enable the rapid deceleration needed as well as allowing decreasing the operating voltage. The device of Xie et al. for example was operated at a membrane-target distance of 2.5 cm and the deceleration at the droplet trajectory as a result was $\sim 5000g$ instead of the $1g$ of Kelvin's thunderstorm [9].

Future developments will aim at confirming the theory developed in reference 11: demonstrating operation at low voltages as well as efficiencies approaching 100%. Another aim will be the development of devices with multiple pores to increase the total current and work towards practical applications.

ACKNOWLEDGEMENTS

Financial support of a NWO TOP Grant (Y.X., A.v.d.B., J.C.T.E.) and the ERC Grant ELab4Life (A.v.d.B.) is gratefully acknowledged. Johan Bomer and Hans de Boer are thanked for technical assistance.

CONTACT

*J.C.T.Eijkel, tel:+31534892839; j.c.t.eijkel@utwente.nl

REFERENCES

- [1] W. Thomson, On a self-acting apparatus for multiplying and maintaining electric charges, with applications to illustrate the voltaic theory. *Proc. R Soc. Lond.* 16, 391–396, 1867
- [2] H.H. Woodson, and J.R. Melcher, *Electromechanical Dynamics, Part II*, pp. 388–392 (Wiley, 1968).
- [3] M. Zahn and H.A. Haus, Contributions of Prof. James R. Melcher to engineering education, *J. Electrostatics* 34, 109–162, 1995
- [4] <https://www.youtube.com/watch?v=els7niCiJrg>
- [5] M.Zahn, Self-Excited AC High Voltage Generation Using Water Droplets, *Amer. J. Phys.* 41, 196–202, 1973
- [6] M. Faubel, and B. Steiner, Strong bipolar electrokinetic charging of thin liquid jets emerging from 10 μm PtIr nozzles, *Ber. Bunsen. Phys. Chem.* 96, 1167–1172, 1992.
- [7] A.M. Duffin, and R.J. Saykally, Electrokinetic hydrogen generation from liquid water microjets. *J. Phys. Chem. C* 111, 12031–12037, 2007
- [8] A.M. Duffin, and R.J. Saykally, Electrokinetic power generation from liquid water microjets. *J. Phys. Chem. C* 112, 17018–17022, 2008
- [9] Y. Xie, D. Bos, L.J. de Vreede, H.L. de Boer, M.-J. van der Meulen, M. Versluis, A.J. Sprenkels, A. van den Berg, and J.C.T. Eijkel, High-efficiency ballistic electrostatic generator using microdroplets, *Nat. Commun.*, 5, 3575, 2014
- [10] Y. Xie, H.L. de Boer, A.J. Sprenkels, A. van den Berg, and J.C.T. Eijkel, Pressure-driven ballistic Kelvin's water dropper for energy harvesting, *Lab Chip* 14, 4171–4177, 2014
- [11] Y. Xie, D. Bos, M.J. van der Meulen, M. Versluis, A. van den Berg, and J.C.T. Eijkel, Ballistic energy conversion: physical modeling and optical characterization, *Nano Energy* 30, 252–259, 2016